CFD aided retail cabinet design

Article *in* Computers and Electronics in Agriculture · May 2002

DOI: 10.1016/S0168-1699(01)00179-X

1 author:

Giovanni Cortella
University of Udine
54 PUBLICATIONS **546** CITATIONS

ELSEVIER

Computers and electronics in agriculture

Computers and Electronics in Agriculture www.elsevier.com/locate/compag
34 (2002) 43–66

CFD-aided retail cabinets design

Giovanni Cortella *

Dipartimento di Energetica e Macchine, Università degli Studi di Udine, via delle Scienze 208, I 33100 Udine, Italy

Abstract

Food requires strict temperature control throughout the so-called 'cold-chain', in which a particular storage temperature is needed for each link. Display cabinets are known to be the weakest link from this point of view and, therefore, particular attention is paid to their design. In this paper, the usefulness of Computational Fluid Dynamics (CFD) is illustrated, as a tool for the prediction of the air flow pattern and of food temperature inside the cabinet. The numerical method is described: the airflow pattern and the load temperature are solved in sequence, in order to save computation time. The results of simulations performed both on a vertical and a horizontal cabinet are reported, as an example of the capabilities of the method. The influence of warm air infiltration on the energy balance of the cabinet is investigated and the results are validated by comparison with experimental tests. The applications reported in this paper showed the model to be reliable, and of valuable help to the designer.

Keywords: Display cabinet; CFD; Food; Cold-chain; Refrigeration

1. Introduction

Most display cabinets in retail stores are forced-air open display cabinets. They have to serve contrasting purposes, i.e. persuading the customer to buy the product, while at the same time preserving it at the adequate temperature. The product must be clearly visible and easy to reach, while it has to be kept as far as possible from the warm shop environment, and from all possible heat sources. To cope with the two contrasting requirements is a difficult task and the display cabinet manufacturer must find the right balance by means of an optimisation process that increases

* Tel.: +39-0432-558022; fax: +39-0432-558027.
E-mail address: giovanni.cortella@uniud.it (G. Cortella).

0168-1699/02/$ - see front matter
PII: S0168-1699(01)00179-X

the technological content of the equipment. However, though improvements have been made in the last 20 years, it is still hard to maintain correct storage temperatures in such refrigerators. Furthermore, their performance in terms of food temperature is strongly affected by ambient conditions. Slight changes in the room temperature, and particularly in its air circulation and radiative heat flux, cause considerable differences in the load temperature. Each cabinet should be certified to comply with the Standard in force for a particular climate class and, once installed in the retail store, it should be kept at the climate conditions as defined in the Standard (ASHRAE Standard, 1983, 1992; DIN Standard, 1978; EN Standard, 1996, 1999; ISO Standard, 1973, 1974, 1979, 1980). However, lighting or forced-air heating and conditioning in the retail store can induce changes in the performance of the cabinet and, therefore, in the temperature of the food.

A great deal of literature has become available since the first papers in 1960–1970 (like those of Gac and Biessy, 1969; Barrillon, 1969), but only in recent years the availability of methods for predicting the air flow patterns and the food temperature has deeply changed the way to the solution of the problem.

The use of CFD for the prediction of the performance of display cabinets in terms of both food temperature and energy consumption has actually became a very useful tool for a better and cheaper design of such units. This is the aim of the work presented in this paper: a computer code written at the University of Udine is illustrated and is applied to the calculation of the airflow pattern and of the food temperature in a vertical and a horizontal display cabinet. A particular approach is followed, since the airflow pattern and the food temperature are estimated separately and in sequence. The method has proven to be reliable also in applications other than display cabinets and can be successfully applied to other processes in food technology.

2. The open retail display cabinet

Open display cabinets for chilled and frozen food are classified by adopting various criteria (IIR, 1986; Gac and Gautherin, 1987; Rigot, 1990; The Refrigerated Food Industry Confederation, 1994; ASHRAE Handbook, 1998; Polonara and Cortella, 2000). The most common criteria are cabinet geometry and product display. In this case, open display cabinets can be of horizontal (open-top, single-deck) or vertical (multi-deck) type.

Horizontal open-top display cabinets (Fig. 1) are the classical appliance for selling frozen foods: the merchandise is stacked from the floor of the unit, and due to cold air stratification, the infiltration of ambient air is relatively insignificant. The heating load is represented mainly by radiative heat transfer from the surroundings and by convective and conductive heat transfer through the walls of the case. Cold air distribution over the stacked product is guaranteed by forced circulation or, less often, by natural convection. Air is extracted through a grill near the top opening (on one side) and forced, by means of fans, through air ducts around the refrigerated compartment to a heat exchanger where it is cooled. Finally, the air is

forced through a symmetrical supply grill on the other side of the opening. The circulating cold air refrigerates the compartment and helps to limit the infiltration of air from the room.

Horizontal cabinets can be equipped with sliding doors, advantageous in terms of reduction of air infiltration, but unattractive for the customers.

Vertical cabinets are the classical appliance for selling chilled food: they are multi-decked (ranging from 2 to 6) in order to save on space and in terms of their display function, they are the most suitable (Fig. 2). The open front is a source of ambient air infiltration, which can be limited by providing one or more (up to three) parallel air curtains. However, due to the irregularities of flow, a more or less significant amount of ambient air is always entrained, reducing the temperature control capabilities and increasing the energy consumption. In an open vertical cabinet, the forced air circulation is very different. Air is extracted through a linear grill at the base of the opening and fans then force it through the cooling coil situated underneath the bottom or behind the back of the load volume. The cooled air is forced to a supply plenum located behind the compartment. A small fraction of the air is sometimes fed into the unit through a perforated plate at the back of the cabinet, while the bulk of the cold air is blown through one or more diffusers situated in front of the canopy.

Vertical display cabinets can also be equipped with glass doors. The performance of such units is not strongly influenced by the room climate conditions, however, each opening of the door leads to a vigorous heat and mass exchange with the ambient air. The simulation of the air flow pattern in vertical closed cabinets is much more complex when taking into account door openings, which is usually not performed.

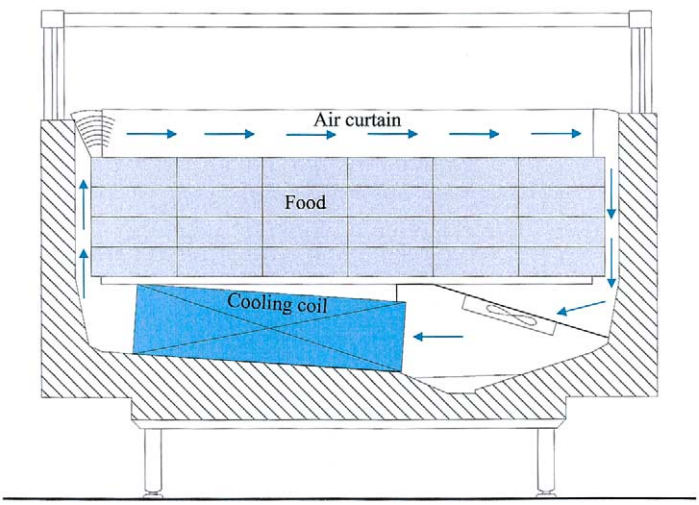

Fig. 1. Cross section of a horizontal open-top display cabinet.

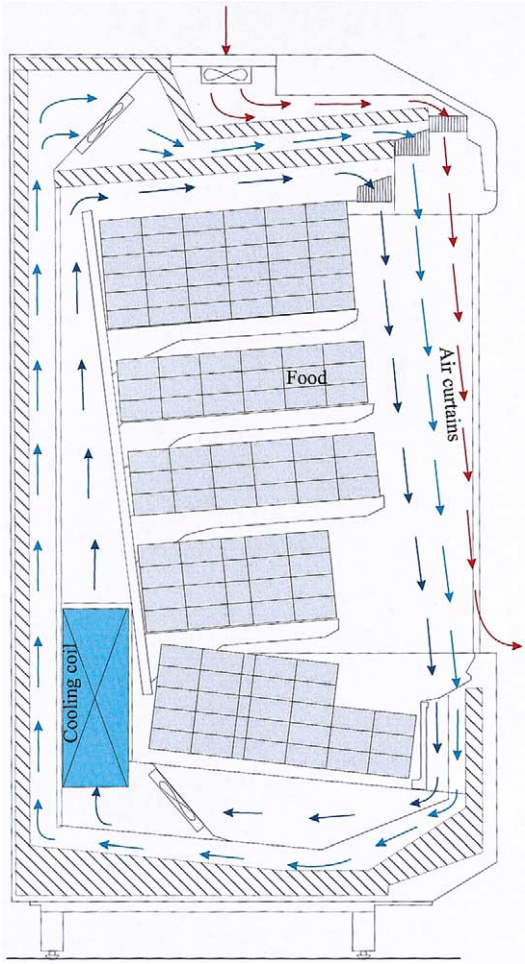

Fig. 2. Cross section of a vertical multi-deck display cabinet.

To achieve the best design of a display cabinet, it is essential to know its thermal energy balance, i.e. all the heat exchanges between the load and the room environment. It depends on several heat sources outside the compartment, or other heat sources close to the load itself (Billiard and Gautherin, 1993). Looking at open cabinets, the contribution of the heat exchange with the ambient by conduction through the cabinet walls is usually negligible, because the walls are made of sandwich panels that are usually well insulated. An unavoidable infiltration of warm air occurs instead through the opening. The air curtain is effective to some degree in open-top horizontal cabinets, where stratification of the cold air helps to minimise any mingling of warm air from the outside and the refrigerated air inside the cabinet; but in vertical cabinets, the creation of a barrier to the incoming warm air remains a crucial problem. A further important heat source from the outside

environment, is the radiative heat exchange between the refrigerated compartment and the walls, ceiling and lighting in the surrounding room (Nesvadba, 1985). Heat exchange by radiation is governed by the emissivity of the bodies. Usually, both the food packages and the walls of the room have a high emissivity of approximately 0.8–0.9, thus leading to high rates of radiative heat flux. Heat gains from internal sources are primarily due to lighting and defrosting devices. Defrosting devices are installed in all cabinets, aiming to keep the air ducts and cooling coils clear of ice. Further sources of heat can be found in additional electric heaters fitted into the rim around the top of horizontal cabinets, which might come into contact with the customers' hands and feel unpleasant if particularly cold.

The radiative heat transfer can be reduced by lowering the emissivity of food packages using materials, such as aluminium, or by using reflective shields (Faramarzi and Woodworth-Szieper, 1999). Heat from lighting can be reduced by replacing incandescent floodlights with fluorescent tubes, and by restricting illumination to a maximum value of 600–700 lux. Air exchange with the room, in the case of open cabinets, can be reduced by controlling the climate conditions in the store and by a better air curtain design.

3. How CFD can contribute to display cabinets design

The main research topic in the design of open display cabinets is the optimisation of the refrigerated air flow which, in turn, is strongly influenced by a large number of parameters, such as the geometry of the unit, the air velocity and the load arrangement (Camporese et al., 1991; Gautherin and Srour, 1995; Howell et al., 1999). In this context, numerical methods for the prediction of the flow pattern are of great interest, since modelling is much more time and cost effective than experimental testing. Furthermore, the Computational Fluid Dynamics (CFD) technique can be used also for the computation of the load temperature. However, the two problems must be investigated separately, due to the very different time constants of the transient phenomena involved.

In the calculation of the air flow pattern, time steps in the range of fractions of seconds are needed, since the air velocity ranges from 0.1 to 1.5 m s^{-1} and the velocity and temperature fluctuations are very fast. In this case, simulations covering an actual time of about 1 min are adequate to give average values of air temperatures and mass and energy flow rates. As an example, in Fig. 3 the calculated temperature at the return duct of a frozen food cabinet is reported together with its average value, for a simulation of 20 s actual time.

When calculating the load temperature, slow changes are encountered due to the much higher heat capacity, and the whole period of time between two defrosting operations (8–12 h typically) must be considered in the simulation. As an example, in Fig. 4 the measured temperature of two packages of food at different locations in the load volume is reported, in the case of one defrosting operation every 12 h. In spite of the great heat capacity of the load, the influence of defrosting on food temperature is clear.

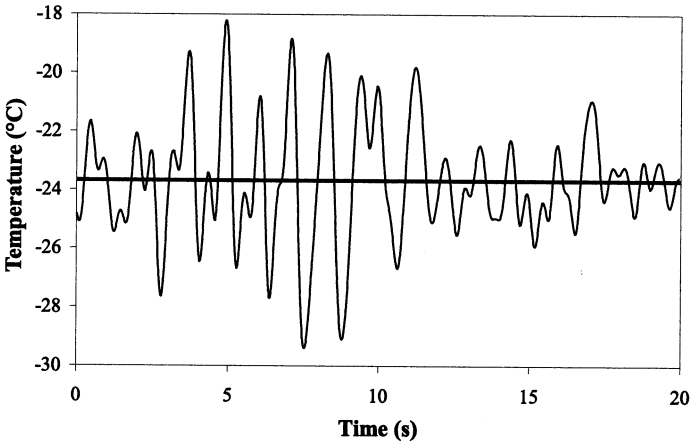

Fig. 3. Calculated air temperature at the return duct in a display cabinet for frozen food.

In this paper, the use of CFD for both the computation of air flow pattern and load temperature is illustrated. The simulation of the air flow pattern is more significant for the manufacture; however, the actual operating conditions of a display cabinet can hardly be reproduced. Too many factors (i.e. the geometry, the position of shelves, the inlet air mass flow rate and temperature, the load and ambient temperature among the most important) act simultaneously and affect each other. Also the influence of radiative heat transfer and of air movements in the ambient should be considered, leading to a very complex model with an almost unpredictable accuracy. For this reason, it is preferable to study a simplified model, with important assumptions like, for example that air stays still in the ambient. In

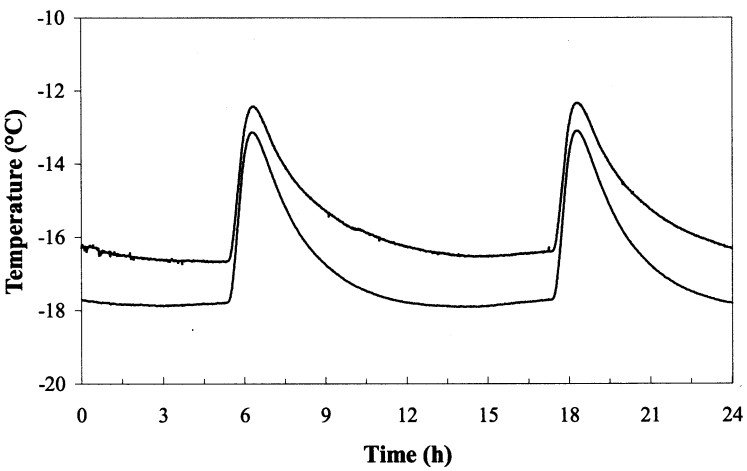

Fig. 4. Measured temperature of two food packages at different locations in a display cabinet for frozen food.

this particular case, the simulation can be performed on the median vertical section, thus disregarding extremity effects which, on the other hand, are recognised to be negligible in cabinets of usual lengths. A 2-D model can be set up, limiting the use of 3-D codes in the case of transversal air movements in the ambient being investigated. The model must in any case be validated by experimental tests, and then can be successfully used for systematic investigations of the influence of geometric parameters or of operating conditions.

When simulating the air flow pattern, the load can be considered as a solid surface (or a body, in 3-D) at a constant temperature, due to the very short duration of the simulation. Once the air flow pattern has been established, the heat transfer coefficients between the load and the air can be computed. This information becomes an input for the estimation of the load temperature, performed with a different computer code. In this case, a transient simulation is still needed, but a very simple coupled conduction-convection code can be used, in which also radiative heat transfer can be reproduced. The food temperature distribution of the load in the cabinet is obtained as a function of time. The defrosting period can also be reproduced by changing the operating conditions (air temperature and mass flow rate) during the simulation.

In the following sections the two models are discussed in more detail.

4. Computation of air flow pattern

The availability of commercial software has remarkably increased the application of CFD to design issues (Van Oort and Van Gerwen, 1995; Baleo et al., 1995; Morillon and Penot, 1996; Stribling et al., 1997; Cortella et al., 1998; Foster and Quarini, 1998; Schiesaro and Cortella, 1999; Foster, 1999). In this paper, for the computation of the air flow pattern a two-dimensional CFD code written at the Dipartimento di Energetica e Macchine of the University of Udine is illustrated. The finite element method and a sequential procedure are employed to discretise and solve the governing differential equations, based on the streamfunction–vorticity formulation. At each solution step, a global energy balance is established by post-processing the energy equation. The software has been successfully validated in previous studies by solving the most relevant benchmark problems (Comini et al., 1994, 1995a, 1996, 1997; Comini and Cortella, 2000).

The code is written for a constant-property Boussinesq fluid, with 2-D incompressible, turbulent flows. In this case, the streamfunction and vorticity equations can be written as:

$$\frac{\partial^2\psi}{\partial x^2}+\frac{\partial^2\psi}{\partial z^2}=-\omega \tag{1}$$

and

$$\frac{\partial\omega}{\partial\vartheta}+u\frac{\partial\omega}{\partial x}+w\frac{\partial\omega}{\partial z}=\frac{\partial}{\partial x}\left(\nu\frac{\partial\omega}{\partial x}\right)+\frac{\partial}{\partial z}\left(\nu\frac{\partial\omega}{\partial z}\right)+g\beta\frac{\partial t}{\partial x} \tag{2}$$

respectively. In Eq. (1) and Eq. (2), ψ is the streamfunction, t is the temperature, β is the coefficient of thermal expansion, x and z are Cartesian co-ordinates defined in such a way that the x-axis is horizontal while the z-axis is vertical (but oriented in the direction opposite to the gravity vector), ϑ is the time and the effective kinematic viscosity is the sum of laminar and turbulent contributions given as (Lardat and Ta Phuoc, 1995; Saro et al., 1998):

$$v = v_l + v_t \tag{3}$$

The velocity components, in the x and z directions, respectively, from the definitions of ψ are:

$$u = \frac{\partial \psi}{\partial z} \tag{4}$$

and

$$w = -\frac{\partial \psi}{\partial x} \tag{5}$$

while

$$\omega = \frac{\partial w}{\partial x} - \frac{\partial u}{\partial z} \tag{6}$$

is defined as the vorticity. The effective thermal diffusivity is the sum of laminar and turbulent contributions

$$a = a_l + a_t \tag{7}$$

In the absence of volumetric heating and neglecting the effects of viscous dissipation, the turbulent energy equation is then:

$$\frac{\partial t}{\partial \vartheta} + u\frac{\partial t}{\partial x} + w\frac{\partial t}{\partial z} = \frac{\partial}{\partial x}\left(a\frac{\partial t}{\partial x}\right) + \frac{\partial}{\partial z}\left(a\frac{\partial t}{\partial z}\right) \tag{8}$$

In this code different turbulence models can be implemented. In the current study, a large eddy simulation procedure (LES) is used, estimating the turbulent fluxes on the basis of the vorticity transfer theory. In accordance with this approach, the turbulent kinematic viscosity is computed as:

$$v_t = (C\Delta)^3\left[\left(\frac{\partial \omega}{\partial x}\right)^2 + \left(\frac{\partial \omega}{\partial z}\right)^2\right]^{1/2} \tag{9}$$

where the average dimension of the element

$$\Delta = (\Delta_x \Delta_z)^{1/2} \tag{10}$$

is the local cut-off length of the filter, while, for isotropic turbulence, the dimensionless constant $C = 0.2$ can be satisfactorily used. Finally, by assuming:

$$\mathrm{Pr}_t = \frac{v_t}{a_t} = 1 \tag{11}$$

the turbulent thermal diffusion is estimated once the turbulent kinematic viscosity is known.

The correct application of boundary conditions is a crucial matter for CFD codes. Different boundary conditions are taken into consideration in the following, covering the needs for a complete reproduction of actual display cabinets operating conditions.

- Solid boundaries: streamfunction and temperature have constant values (conditions of the first kind).
- Inflow boundaries: the temperature has a constant value; the streamfunction increases according to its definition.

$$\psi(s) - \psi_0 = \int_0^s u_n(s)\mathrm{d}s \tag{12}$$

where u_n is the inlet velocity, i.e. the normal component of the velocity vector at the inlet boundary. In this way, any inlet velocity profile can be imposed by the appropriate streamfunction variation. At solid and inflow boundaries a boundary condition can be applied also to the normal derivative of the streamfunction, which is known to be:

$$\frac{\partial \psi}{\partial n} = u_s \tag{13}$$

where u_s is the tangential velocity component equal to zero on solid boundaries. In the solution process, this additional information on the tangential velocity component is used as numerical boundary condition when the vorticity field is computed, as illustrated by Comini et al. (1994, 1995a, 1997).

- Open boundaries: the temperature of the incoming fluid is known and constant; the temperature of the fluid exiting the domain satisfies a zero gradient boundary condition:

$$\frac{\partial t}{\partial n} = 0 \tag{14}$$

The vorticity of the incoming fluid can be set equal to zero, while the vorticity of the fluid going out of the domain satisfies the zero gradient boundary condition:

$$\frac{\partial \omega}{\partial n} = 0 \tag{15}$$

The streamfunction, for both incoming and exiting flows, satisfies the natural boundary condition:

$$\frac{\partial \psi}{\partial n} = 0 \tag{16}$$

There is a further condition on streamfunction, deriving from its definition, similar to Eq. (12) and making reference to the normal component of the velocity vector at the open boundary:

$$\frac{\partial \psi}{\partial s} = u_n \tag{17}$$

Through this boundary condition we can discriminate between incoming flows ($u_n > 0$) and exiting flows ($u_n < 0$).

The resulting differential equations are discretised following a finite element method. First, a Bubnov–Galerkin procedure is implemented, then a fully implicit time stepping scheme is applied to the space-discretised versions of the equations. Final systems of algebraic equations are obtained, which are solved in sequence, taking special care to properly compute the values of the vorticity at solid and inflow boundaries. The procedure is well illustrated in Comini et al. (1994, 1995a, 1997) for laminar flows.

The rates of heat flow through the solid walls can be computed, in order to know the heat flux from the load and then estimate the heat transfer coefficients. For this purpose, the discretised energy equation can be post processed, and the heat flux rates computed from the reactions at those nodes where temperature boundary conditions of the first kind are imposed, as detailed in Comini et al. (1995a).

For the application of this method to display cabinets, a computational domain has to be identified. Usually, the domain consists of the whole load volume of the cabinet, taking into account the presence of food, and including a portion of the external ambient, in order to visualise the air overspilling from the cabinet to the floor. The domain is then subdivided into elements, quadratic of the parabolic type (eight nodes each). The maximum number of elements required for our simulations on display cabinets is about 2500, corresponding to about 8000 nodes. With such a domain, the computational time on a 500 MHz personal computer is of about 1 hour every 10 s of actual time, corresponding to 1000 steps (the time step is 0.01 s). The numerical solution does not achieve a steady state, or even a periodic regime and, consequently, the calculations must be stopped when the time-averaged value of the return air temperature does not vary with time any more, i.e. after 40–60 s of actual time.

It should be noted that the computer code here utilised is not optimised with respect to computational time, since it is usually applied to domains with no more than 10 000–15 000 nodes.

4.1. Application to vertical cabinets

Fig. 5 shows a schematic cross section of a fully loaded vertical display cabinet with the corresponding computational domain. The results of the simulation can be given in terms of heat balance (i.e. refrigerating power needed, heat infiltration from the ambient, heat flux from the food), or air temperature field. In this case, the results can be conveniently displayed by temperature maps, obtained using different colours or grey tones. An example of a temperature map is given in Fig. 6, referring to the computational domain of Fig. 5. The air curtains move downwards at the front of the cabinet because of their velocity and buoyancy forces until a strong fluctuation entrains the warm room air. The total mass flow rate thus increases and, after extraction from the grill at the base of the cabinet, a significant portion of refrigerated air overspills onto the floor as a result.

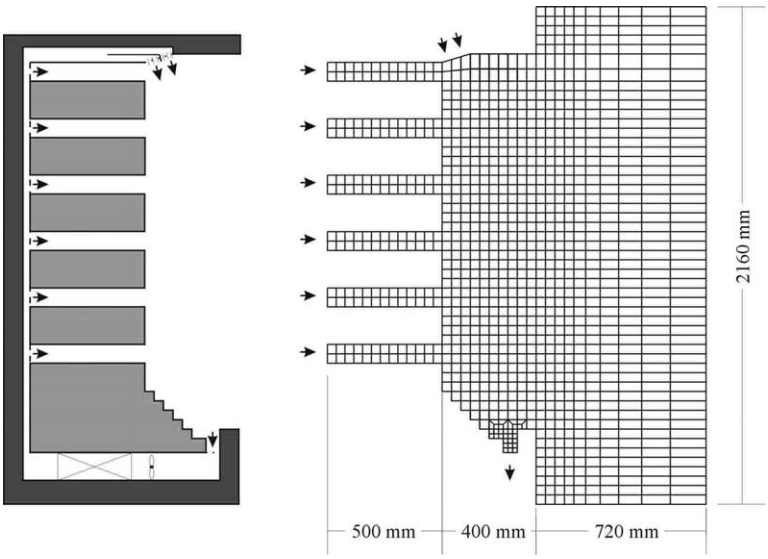

Fig. 5. Schematisation of a vertical multi-deck display cabinet, and corresponding computational domain for the air flow pattern simulation.

Fig. 6 represents the temperature field calculated at a particular time; similar maps, calculated at each time step, can be suitably sequenced, spaced in time, in order to show typical velocity and temperature fluctuations, since they do not achieve a steady state, or even a periodic regime. An example of such a representation is given in Fig. 7, while an example of animation in .mpg format can be obtained from the author upon request.

The validation of this method has been done by comparison with tests performed on various display cabinets, in a test room in compliance with the EN441 Standard. The main objective of the investigation was always the reduction of external air infiltration and of energy consumption.

In the work of Schiesaro and Cortella (1999) the CFD technique has been applied to the design of three air curtains in a vertical frozen food display cabinet. This application was of great interest, since vertical open cabinets are typically used in Europe only for chilled food. Various values of the air velocity were assumed for the air curtains, looking for the operating condition yielding the lowest external air entrainment. A particular configuration was selected and tested for validation, revealing the validity of the simulation. In fact, when reproducing the experimental tests with a correct choice of the simplified model, an excellent agreement was found between the simulated and measured power requirement, air velocity and air temperature values, as reported in Table 1.

In Cortella et al. (2001) the results of a similar work are illustrated, which were performed on a vertical open display cabinet for chilled food with two air curtains. As a performance criterion for the comparison of different configurations, the efficiency of the air curtains was defined as:

Table 1
Results of validation of the simulation model of a vertical display cabinet for frozen food

	Air curtain mean velocity ($m\ s^{-1}$)[a]			Air curtain mean temperature (°C)			Return air grill mean temperature (°C)		Refrigerating power ($W\ m^{-1}$)
	Internal	Central	External	Internal	Central	External	Internal	External	
Experimental	1.74	1.42	0.80	−24.2	+1.2	+25.6	−17.6	+4.1	2018
Computed	1.74	1.42	0.80	−24.1	+1.0	+28.0	−16.4	+4.9	1943

[a] Air velocity in the model is imposed equal to the measured values.

Table 2
Influence of air infiltration on the energy balance of a vertical display cabinet for chilled food, at various values of the air curtain velocity

Inner curtain velocity ($m\ s^{-1}$)	Outer curtain velocity ($m\ s^{-1}$)	Refrigerating power ($W\ m^{-1}$)	Heat flux from the load ($W\ m^{-1}$)	Heat flux due to air infiltration ($W\ m^{-1}$)	Air curtain efficiency (−)
0.30	0.30	616	129	487	0.21
0.30	0.65	675	123	552	0.18
0.30	1.00	714	135	579	0.19
0.65	0.30	788	126	662	0.16
1.00	0.30	1009	141	868	0.14

$$\text{Air curtain efficiency} = \frac{\text{Heat flow rate from the load}}{\text{Total refrigerating power}} \quad (18)$$

Table 2 shows the values reported in the above cited paper, in which the influence of the air curtain velocity is clear.

Various experimental techniques can also be implemented for the investigation of the air flow pattern in display cabinets, such as Laser Doppler Anemometry (LDA) (Foster, 1999) and tomographic imaging (Penot et al., 1995, 1999). However, the benefit of the use of CFD is clear in terms of both time and money savings, and such experiments can be performed for a final check of the correctness of numerical results.

4.2. Application to horizontal cabinets

Horizontal cabinets are much more energy efficient and effective in terms of their preserving function. Cold air stratification occurs on the open top, thus limiting

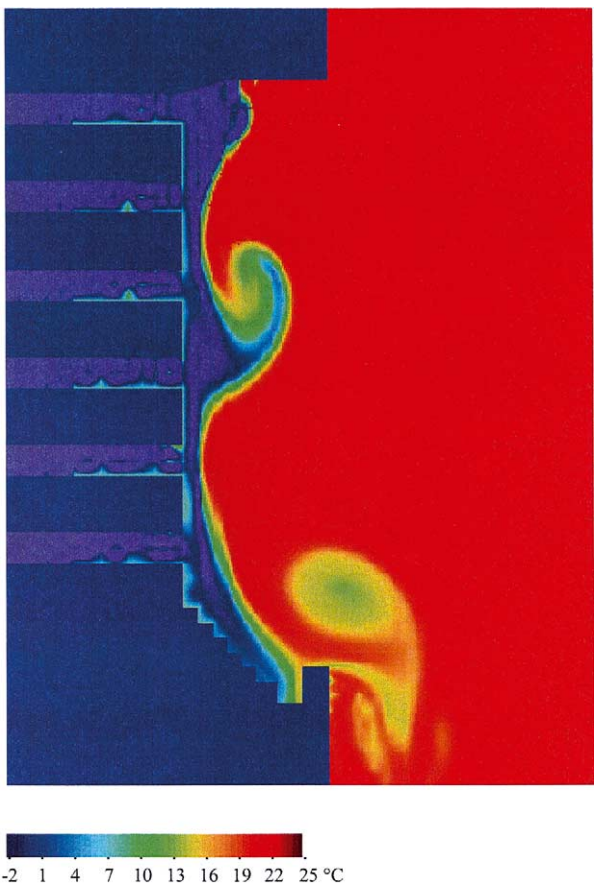

Fig. 6. Calculated temperature map of the air flow pattern in a vertical display cabinet.

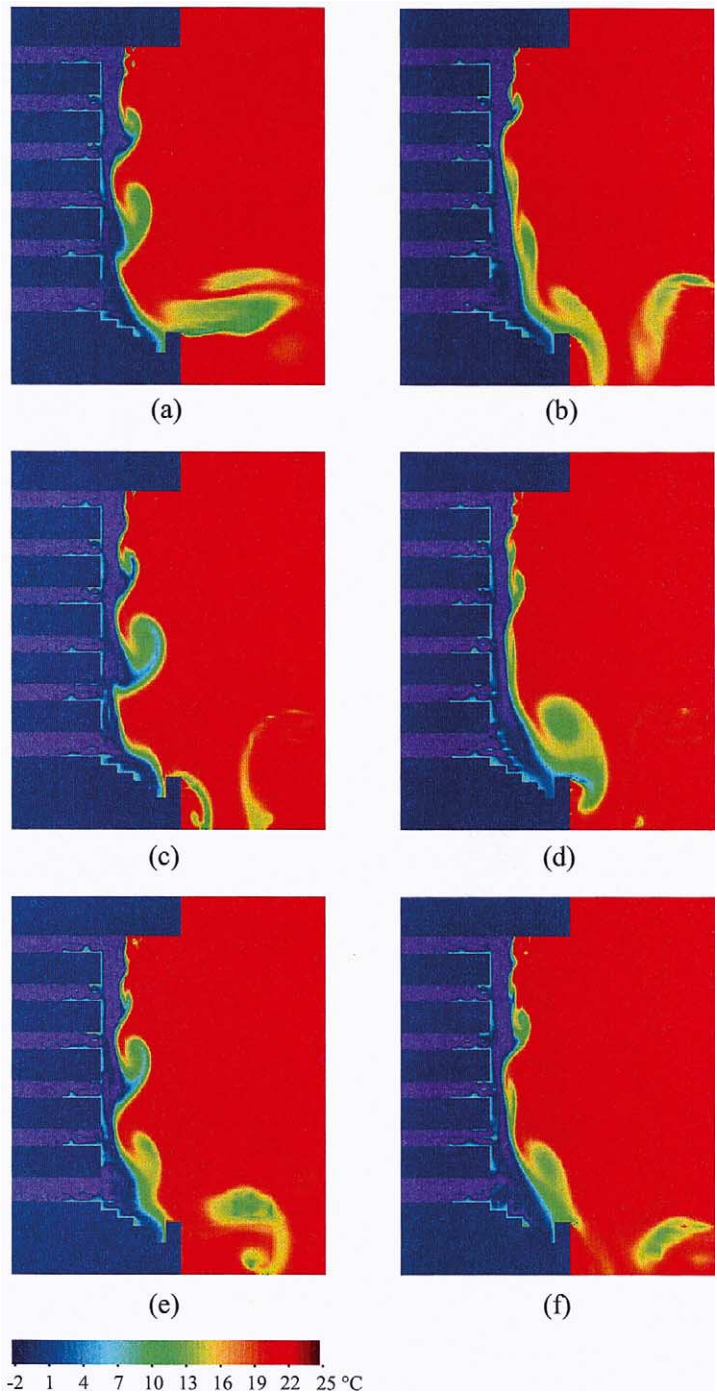

Fig. 7. Sequence of temperature maps of the air flow pattern in a vertical display cabinet, at 1 s time step.

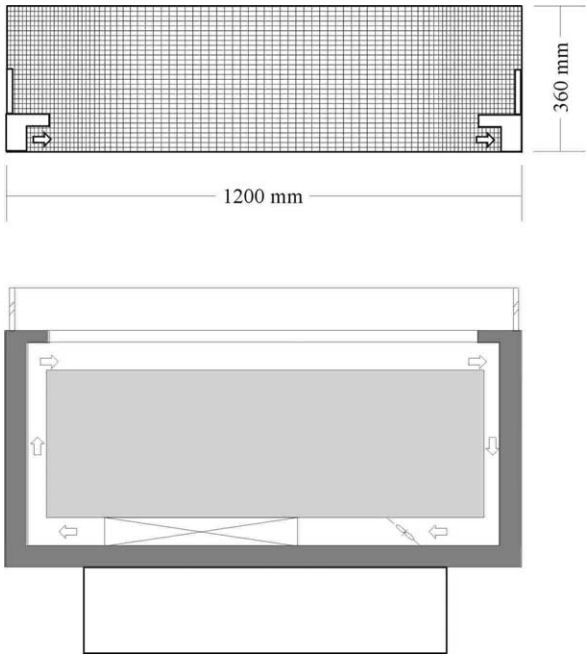

Fig. 8. Schematisation of a horizontal open top display cabinet, and corresponding computational domain for the air flow pattern simulation.

warm air entrainment from the outside. However, refrigerated air velocity strongly influences the performance of the unit: if the air velocity is too low, the necessary refrigerating effect (and consequently the correct storage temperature) cannot be guaranteed; if the air velocity is too high, the air stream becomes more turbulent, thus increasing heat and mass transfer with the environment. For this reason, CFD simulations are very useful also for this kind of cabinets.

The procedure is the same as for vertical units: a computational domain is identified, including the volume where the horizontal air curtain takes place and a portion of the external environment. Fig. 8 illustrates a schematic view of a horizontal cabinet with the corresponding computational domain, which comprises the zone where air flows over the load, including a portion of the external environment.

The simulation is performed with the same objective: the reduction of external air entrainment, and the investigation of the influence of the operating conditions on the air flow pattern. As an example, in Fig. 9 the temperature maps obtained at various values of the forced air velocity are reported (Cortella et al., 1998). The influence on the flow pattern is clearly visible. At the highest velocity the flow becomes very turbulent, and strong recirculation zones are created. In this situation, the heat and mass transfer with ambient increase, and greater intake of ambient air leads to an early frosting of the cooling coil and to a rapid decay of the cabinet performance (Bobbo et al., 1995).

The results of the simulation of the air flow pattern of both vertical and horizontal cabinets can be processed for the estimation of the convective heat transfer coefficients between air and the load surface. This information is necessary to the second part of the display cabinet simulation: the computation of food temperature.

5. Computation of food temperature

The estimation of the load temperature is a coupled conduction–convection problem. Heat is transferred through the solid and convective boundary conditions with specified convection coefficients and fluid temperatures are imposed. By using an appropriate computer code, the detailed temperature distributions in the solid and the variation of the bulk temperature in the fluid can be computed.

The finite element formulation here proposed has been developed by Comini et al. (1993), and has been utilised to solve various problems linked to food refrigeration, such as refrigerated transport (Comini et al., 1995b) and horizontal display cabinets (Bobbo et al., 1995). The mathematical model and the finite element formulation are detailed in Comini et al., (1995b). Therefore, here only the basic elements of the method are described.

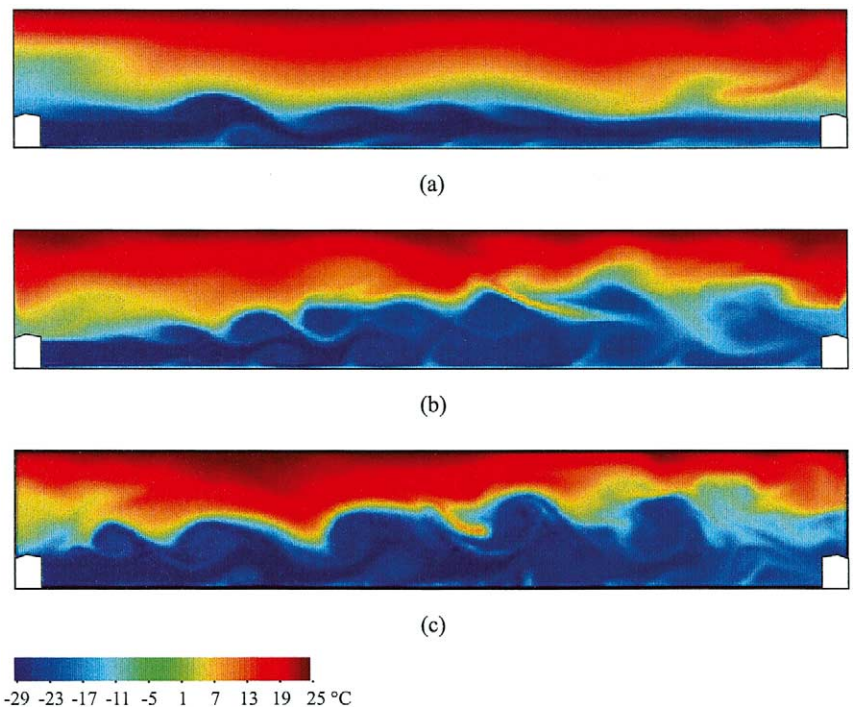

Fig. 9. Calculated temperature maps of the air flow pattern in a horizontal display cabinet at various values of the air velocity: (a) 0.2 m s^{-1}, (b) 0.3 m s^{-1}, (c) 0.4 m s^{-1}.

In 2-D problems, the heat conduction equation for the solid regions is:

$$\rho c \frac{\partial t}{\partial \vartheta} = \frac{\partial}{\partial x}\left(k \frac{\partial t}{\partial x}\right) + \frac{\partial}{\partial y}\left(k \frac{\partial t}{\partial y}\right) + \dot{q} \tag{19}$$

where t is the temperature, k is the thermal conductivity, supposed uniform in the solid, ρc is the heat capacity per unit volume, $\dot{q}$ is the rate of internal heat generation per unit volume, x and y are Cartesian co-ordinates and ϑ is the time. In order to properly take into account the contributions from the fluid, assuming the average inlet fluid velocity u_f and the average convection coefficient h, the energy equation is:

$$\rho_f c_f \delta_f \left(\frac{\partial t_f}{\partial \vartheta} + u_f \frac{\partial t_f}{\partial s}\right) = \frac{\partial}{\partial s}\left(k_f \delta_f \frac{\partial t_f}{\partial s}\right) - h(t_f - t_w) \tag{20}$$

where s is the axial co-ordinate, k_f is the fluid thermal conductivity, and δ_f is the width of the flow passage, whose length is $l \gg \delta_f$.

The boundary conditions for Eq. (19) can be of prescribed temperature:

$$t = t_p \tag{21}$$

of prescribed heat flux:

$$q''_p = -k \frac{\partial t}{\partial n} \tag{22}$$

of prescribed convective heat exchange with a fluid at temperature t_e:

$$h(t - t_e) = -k \frac{\partial t}{\partial n} \tag{23}$$

The problem is solved through a finite element discretisation; the unknown temperature in the whole domain is approximated by means of the expansion:

$$t \cong \sum_{j=1}^{n} N_j(x, y) t_j(\vartheta) = N\boldsymbol{t} \tag{24}$$

where N_j are the shape functions. Eqs. (19) and (20) are discretised with respect to the space variables through the weighted residual method. The residuals, obtained by substituting Eq. (24) into Eq. (19) and Eq. (20), are weighted by means of suitable functions W_j equal to N_i in the solid (Bubnov–Galerkin formulation) or of the upwind type in the fluid (Petrov–Galerkin formulation).

The final set of ordinary differential equations is:

$$\boldsymbol{C}\dot{\boldsymbol{t}} + \boldsymbol{K}\boldsymbol{t} = \boldsymbol{s} \tag{25}$$

where $\boldsymbol{C}$ is the capacity matrix, $\dot{\boldsymbol{t}}$ is the time derivative of the temperature $\boldsymbol{t}$, $\boldsymbol{K}$ is the matrix sum of homogeneous contributions and $\boldsymbol{s}$ is the vector sum of non-homogeneous contributions. With constant $\boldsymbol{C}$, $\boldsymbol{K}$, $\boldsymbol{s}$ a standard finite difference scheme can be implemented for the integration of Eq. (25), following a fully implicit scheme.

In some cases with regular geometry, the element matrices and vectors related to fluid and surface convection can be expressed in closed form with algebraic

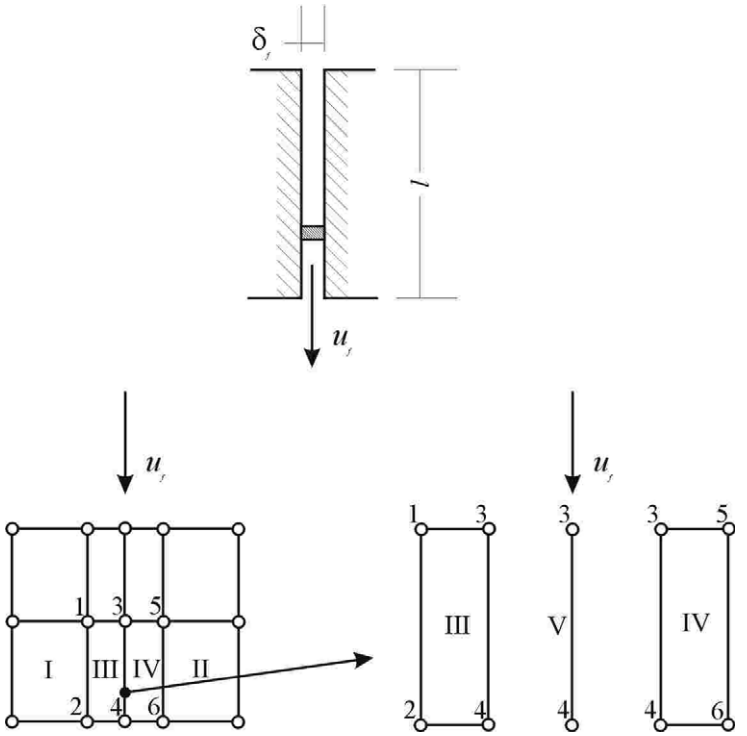

Fig. 10. Scheme of surface convection in case of fluid flowing in a narrow channel.

expressions, provided that linear shape and weighting functions are used. Consider the situation of Fig. 10, where we have both fluid and surface convection contribution from the fluid flowing in a narrow channel. We can use a fluid convection element V between the surface convection elements III and IV. In this way, the surface convection elements take into account the energy exchanges between the solid surfaces and the fluid, while the fluid convection elements take into account the additional contributions to the energy balance due to the bulk motion of the fluid (Comini et al., 1993).

This method can be applied to the evaluation of the food temperature in display cabinets, once the boundary conditions for the load are identified. Three boundary zones can be distinguished: the insulated walls (vertical walls and part of the bottom), the bottom wall adjacent to the cooling coil and the open top.

The insulated walls can be schematised as in Fig. 11: the load volume is delimited by a thin metal wall, and a cavity for forced air circulation is created among this wall and the external insulating panel.

In Fig. 11, two heat transfer coefficients have to be assumed:

$h_{\mathrm{eq(air\rightarrow room)}}$, due to the heat transfer from the fluid through the insulated panel to the room, and

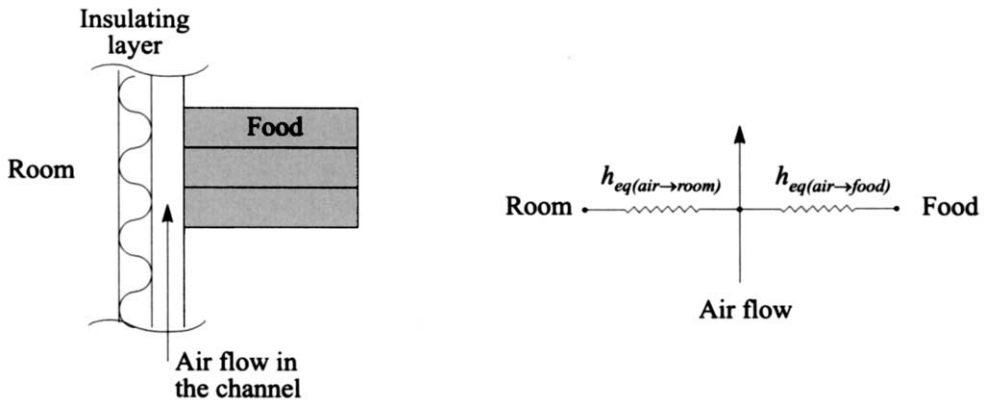

Fig. 11. Model of the insulated walls of the load volume in a horizontal display cabinet.

$h_{eq(air \rightarrow food)}$, due to the heat exchange from the food to the air flow, which must be computed from the well established theory of conduction and convection.

At the bottom wall adjacent to the cooling coil an average equivalent convection coefficient can be applied, including the combined effects of conduction and of thermal contact resistance, being the food in direct contact with the cooling surface, through the thin metal wall.

Finally, the open top can be schematised as in Fig. 12: the air curtain flows close to the upper surface of the load, preventing an excessive heat and mass transfer with the ambient. The air curtain fails to reduce the radiative heat transfer, which occurs by radiation from the room surfaces (walls, ceiling) to the food upper surface, and is probably the majority of the global heat transfer (Nesvadba, 1985). With this code, radiative heat transfer is simulated as heat generated on the top of the surface of the first layer of the load.

In Fig. 12, two heat transfer coefficients have to be assumed:

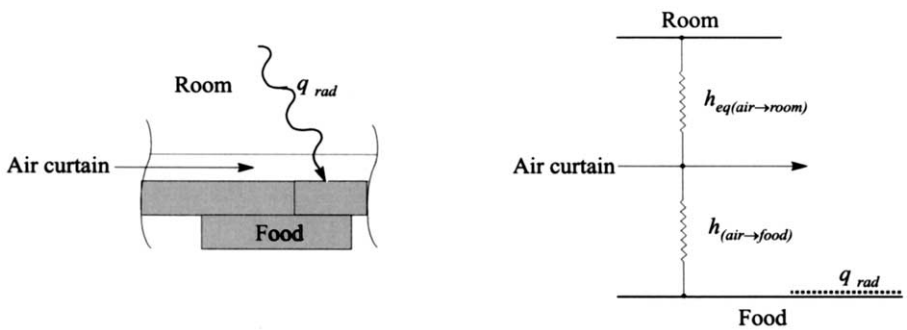

Fig. 12. Model of the open top of the load volume in a horizontal display cabinet.

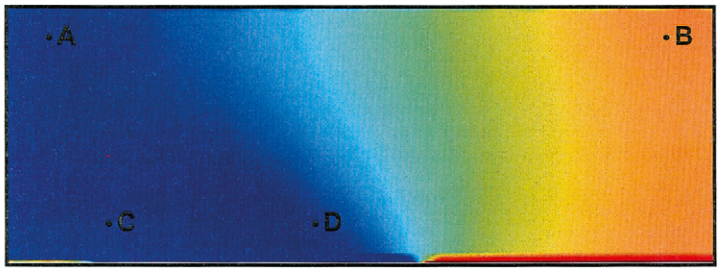

(a)

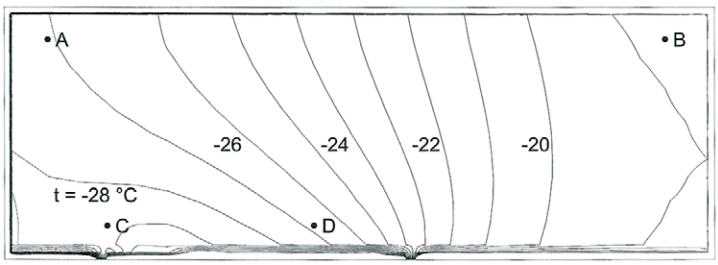

(b)

Fig. 13. Temperature map (a) and isothermal lines (b) of the load in a horizontal display cabinet after the refrigeration period; A, B, C, D are the points where the temperature reported in Fig. 15 is measured.

$h_{(\mathrm{air}\rightarrow\mathrm{food})}$, due to forced convection between the air curtain and the food, whose value can be computed from the air flow pattern simulations, and

$h_{\mathrm{eq(air}\rightarrow\mathrm{room)}}$, due mostly to mass transfer from the air curtain to the room, whose value can be computed from the air flow pattern simulations.

The average temperature of the forced air curtain at the inlet of the computational domain can be assumed from experimental tests, or computed through the preliminary simulation of the air flow pattern.

The simulation is carried out in the transient regime, because we look for changes in food temperature distribution with time. The effect of the defrosting operation (which is usually activated by a timer) can be computed by changing the temperature of the air entering the load volume. The computation time for this application is of about one hour for the simulation of a complete cycle (refrigeration-defrosting) on a 500 MHz personal computer.

As an example, two temperature maps of the load in the cabinet of Fig. 8 are reported in Fig. 13 and Fig. 14. In this case, the simulation is carried out reproducing consecutive cycles, each composed of 11.5 h of refrigeration and 30 min of defrosting, without considering the use of night covers. The refrigerated air is assumed to leave the cooling coil at a temperature $t = -35$ °C during refrigeration and $t = 10$ °C during defrosting.

In Fig. 13 the load temperature distribution in a cross-section of the cabinet at the end of the refrigeration period is illustrated. The effect of the clockwise forced air circulation around the load is evident. The temperature of the packages in the upper layer of the load is strongly dependent on their position, the warmest package being located close to the return air duct. The effect of the cold surface due to the cooling coil on the bottom of the cabinet is also clear.

Fig. 14 illustrates the load temperature pattern at the end of the defrosting cycle. Due to the circulation of warm air and to local heating on the cooling coil, the whole load suffers a rise in temperature. Products in the lower layer undergo a greater temperature change, but the warmest package is always located on the upper surface of the load.

The predicted temperature at any point inside the load volume can be plotted against time. As an example, the temperature of four ideal packages identified by the letters A, B, C and D in Fig. 13 and 14, is plotted in Fig. 15 for a complete 12-h cycle. The initial time $\vartheta = 0$ coincides with the end of the refrigerating period, when the lowest load temperature is reached. During the next 30 min of defrosting, the temperature of the load rapidly rises by 2.5–3.5 °C, due to the lack of refrigeration and to the additional heat load from the defrosting device. The initial temperature pattern is reached again by the end of the subsequent refrigerating cycle.

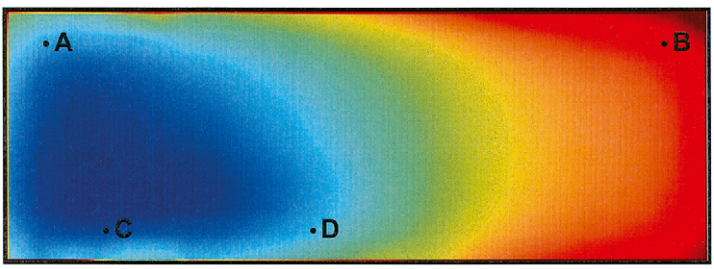

(a)

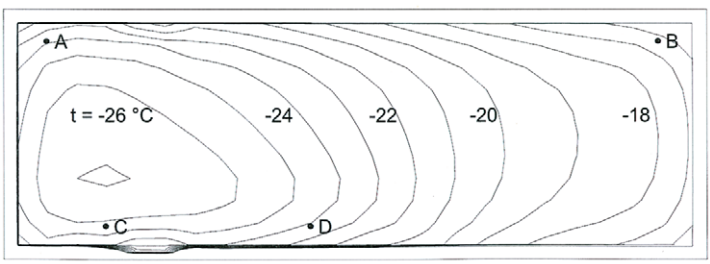

(b)

Fig. 14. Temperature map (a) and isothermal lines (b) of the load in a horizontal display cabinet after the defrosting period; A, B, C, D are the points where the temperature reported in Fig. 15 is measured.

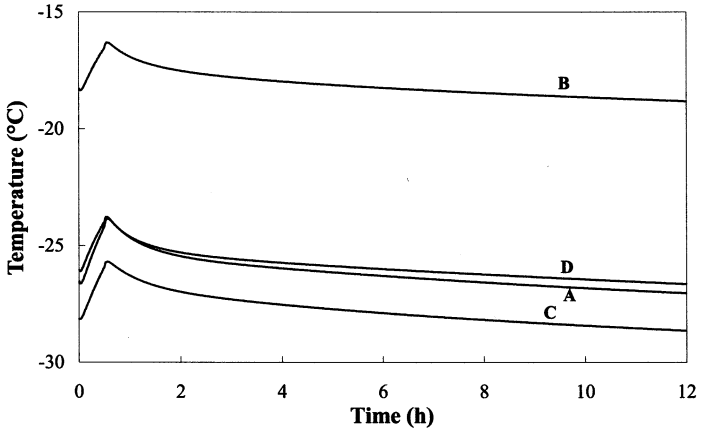

Fig. 15. Predicted load temperature at the four points A, B, C, D identified in Fig. 13 and Fig. 14, during a defrosting + refrigeration cycle.

6. Conclusions

CFD has proved to be a very useful tool at the design stage of refrigerated display cabinets. The influence of many important parameters, such as the geometry of the cabinet, the air curtain velocity and temperature, and the load arrangement, can be rapidly analysed. The few simple models reported in this paper showed to be reliable, and of valuable help to the designer.

It is instead more difficult to obtain quantitatively accurate results with simple models, due to the very complex and often unstable boundary conditions that should be implemented. The performance of display cabinets is strongly affected by room air velocity and temperature, and with such simple models it seems a hard job even to reproduce experimental tests performed in a climatic room, i.e. in very stable and controlled ambient conditions.

However, a few comparative experimental tests are sufficient to validate the results of simulations, that can be successfully used to predict the performance of the cabinet in operating conditions different from the experimental ones.

References

American Society of Heating, Refrigerating and Air conditioning Engineers (ASHRAE), 1998. Retail food store refrigeration and equipment. Handbook 1998 Refrigeration, 47. ASHRAE, Atlanta, USA.

ASHRAE Standard 72/1983R—Methods of testing open refrigerators for food stores.

ASHRAE Standard 117/1992 Methods of testing self-service closed refrigerators for food stores.

Baleo, J.N., Guyonnaud, L., Solliec, C., 1995. Numerical simulation of air flow distribution in a refrigerated display case air curtain. Proc. 19th International congress of refrigeration, IIR/IIF, The Hague, NL, II, pp. 681–688.

Barrillon, D., 1969. Les phénomènes thermiques dans les meubles ouverts pour la vente de produits surgelés. Revue Générale du Froid 5, pp. 697–704.

Billiard, F., Gautherin, W., 1993. Heat balance of an open type freezer food display cabinet. Proc. International conference. Cold chain refrigeration equipment by design, IIR/IIF, Comm B1, B2, D1, D2/3, Paris, pp. 322–332.

Bobbo, S., Cortella, G., Manzan, M., 1995. The temperature of frozen food in open display freezer cabinets: simulation and testing. Proc. 19th International congress of refrigeration, IIR/IIF, The Hague, NL, II, pp. 697–704.

Camporese, R., Cortella, G., Bigolaro, G., Scattolini, M., 1991. Effects of load arrangement on the thermal performance of open display cabinets. Proc. 18th International congress of refrigeration, IIR/IIF, Montréal, IV, pp. 1965–1969.

Comini, G., Cortella, G., 2000. Streamfunction–vorticity formulation of incompressible flow and heat transfer problems. In: Sundén, B., Comini, G. (Eds.), Computational Analysis of Convection Heat Transfer. WIT Press, Southampton, UK, pp. 35–70.

Comini, G., Saro, O., Manzan, M., 1993. A physical approach to finite element modelling of coupled conduction and convection. Numerical Heat Transfer B 24, 243–261.

Comini, G., Manzan, M., Nonino, C., 1994. Finite element solution of the streamfunction–vorticity equations for incompressible two-dimensional flows. International Journal for Numerical Methods in Fluids 19, 513–525.

Comini, G., Cortella, G., Manzan, M., 1995a. A streamfunction–vorticity based finite-element formulation for laminar–convection problems. Numerical Heat Transfer Part B 28, 1–22.

Comini, G., Cortella, G., Saro, O., 1995b. Finite element analysis of coupled conduction and convection in refrigerated transport. International Journal of Refrigeration 18, 123–131.

Comini, G., Cortella, G., Manzan, M., 1996. Natural convection in rectangular open cavities. In: Wrobel, L.C., Comini, G., Brebbia, C.A., Nowak, A.J. (Eds.), Advanced Computational Methods in Heat Transfer, vol. IV. Computational Mechanics Publications, Southampton, UK, pp. 13–22.

Comini, G., Manzan, M., Cortella, G., 1997. Open boundary conditions for the streamfunction-vorticity formulation of unsteady laminar convection. Numerical Heat Transfer Part B 31, 217–234.

Cortella, G., Manzan, M., Comini, G., 1998. Computation of air velocity and temperature distributions in open display cabinets. Proc. International Conference, Advances in the refrigeration systems, food technologies and cold chain, Sofia, pp. 617–625.

Cortella, G., Manzan, M., Comini, G., 2001. CFD Simulation of refrigerated display cabinets. International Journal of Refrigeration 24, 250–260.

DIN Standard 8954—Offene Verkaufskühlmöbel, 1978.

EN Standard 441—Refrigerated Display Cabinets. Parts 1–11, 1996.

EN Standard 441—Refrigerated Display Cabinets. Part 12, 1999.

Faramarzi, R.T., Woodworth-Szieper, M.L., 1999. Effects of low-emissivity shields on the performance and power use of refrigerated display case. ASHRAE Transactions, ASHRAE, Chicago 105 (1), 533–540.

Foster, A.M., 1999. The benefits of computational fluid dynamics for modelling processes in the cold chain. Proc. 20th International congress of refrigeration, IIR/IIF, Sydney, IV, Paper 682.

Foster, A.M., Quarini, G.L., 1998. Using advanced modelling techniques to reduce the cold spillage from retail display cabinets into supermarket stores. Proc. IRC/IIR conference, Refrigerated transport, storage and retail display. Cambridge, UK, pp. 217–225.

Gac, A., Biessy, J.C., 1969. Etude théorique des échanges de chaleur dans un meuble de vente a basse température. Revue Générale du Froid 5, 707–716.

Gac, A., Gautherin, W., 1987. Le froid dans les magasins de vente de denrées périssables. Pyc Edition, Paris.

Gautherin, W., Srour, S., 1995. Effect of climatic conditions on the operation of refrigerating equipment in a hypermarket. Proc. 19th International congress of refrigeration, IIR/IIF, The Hague, NL, II, pp. 705–712.

Howell, R.H., Rosario, L., Riiska, D., Bondoc, M., 1999. Potential savings in display case energy with reduced supermarket relative humidity. Proc. 20th International congress of refrigeration, IIR/IIF, Sydney, IV, Paper 113.

IIR-International Institute of Refrigeration, 1986. Recommendations for the Processing and Handling of Frozen Foods. IIR/IIF, Paris.

ISO Standard 1992—Commercial refrigerated cabinets—methods of test. Parts 1–3, 1973
ISO Standard 1992—Commercial refrigerated cabinets—methods of test. Parts 4–6, 1974
ISO Standard 5160—Commercial refrigerated cabinets—technical specifications. Part 1, 1979.
ISO Standard 5160—Commercial refrigerated cabinets—technical specifications. Part 2, 1980.
Lardat, R., Ta Phuoc, L., 1995. Numerical simulation of turbulent flow around a NACA0012 airfoil at 20° of attack. In: Taylor, A., Durbetaki, A. (Eds.), Numerical Methods in Laminar and Turbulent Flow, vol. 9. Pineridge Press, Swansea, UK, pp. 421–432.
Morillon, C., Penot, F., 1996. La modélisation: une aide à la conception thermoaéraulique des meubles frigorifiques de vente. Revue Générale du Froid 968, 48–53.
Nesvadba, P., 1985. Radiation heat transfer to products in refrigerated display cabinets. Proc. International Conference IIF IIR Commissions C2, D3, Aberdeen, NL, 1985–4, pp. 323–329.
Penot, F., Morillon, C., Mousset, S., 1995. Analyse et numérisation d'images d'écoulements pour l'étude des meubles frigorifiques de vente. Proc. 19th International congress of refrigeration, IIR/IIF, The Hague, NL, II, pp. 106–113.
Penot, F., Mousset, S., Morillon, C., 1999. Tomographic imaging of air curtains in display cabinets compared to thermal measurements. Proc. 20th International congress of refrigeration, IIR/IIF, Sydney, IV, Paper 639.
Polonara, F., Cortella, G., 2000. Retail display equipment. In: Kennedy, C.J. (Ed.), Managing Frozen Food. Woodhead Publishing, Cambridge, UK.
Rigot, G., 1990. Meubles et vitrines frigorifiques. Pyc Edition, Paris.
Saro, O., Manzan, M., Cortella, G., 1998. Finite element analysis of heat transfer from jets impinging on a surface. Proc. 16th Congresso nazionale sulla trasmissione del calore-UIT, Siena, Italy, 2, pp. 559–569 (in Italian).
Schiesaro, P., Cortella, G., 1999. Optimisation of air circulation in a vertical frozen food display cabinet. Proc. 20th International congress of refrigeration, IIR/IIF, Sydney, IV, Paper 174.
Stribling, D., Tassou, S.A., Marriott, D., 1997. A two-dimensional computational fluid dynamic model of a refrigerated display case. ASHRAE Transactions 103 (1), 88–94.
The Refrigerated Food Industry Confederation, 1994. Guide to the Storage and Handling of Frozen Foods, (the Golden Book). British Frozen Food Federation, Grantham, UK.
Van Oort, H., Van Gerwen, R.J.M., 1995. Air flow optimisation in refrigerated cabinets. Proc. 19th International congress of refrigeration, IIR/IIF, The Hague, NL, II, pp. 446–453.